Universität Augsburg

Institut für Mathematik

Michael Fischer, Alexander Vasilyev, Tatjana Stykel, Peter Eberhard

Model Order Reduction for Elastic Multibody Systems with Moving Loads

Preprint Nr. 04/2015 — 17. März 2015

Institut für Mathematik, Universitätsstraße, D-86135 Augsburg http://www.math.uni-augsburg.de/

Impressum:

Herausgeber:

Institut für Mathematik
Universität Augsburg
86135 Augsburg
`http://www.math.uni-augsburg.de/de/forschung/preprints.html`

ViSdP:

Tatjana Stykel
Institut für Mathematik
Universität Augsburg
86135 Augsburg

Model Order Reduction for Elastic Multibody Systems with Moving Loads

Michael Fischer †
Email: michael.fischer@itm.uni-stuttgart.de

Alexander Vasilyev ‡
Email: vasilyev@math.uni-augsburg.de

Tatjana Stykel ‡
Email: stykel@math.uni-augsburg.de

Peter Eberhard †
Email: peter.eberhard@itm.uni-stuttgart.de

In this paper we consider two different model reduction approaches for elastic multibody systems with moving loads. The first approach is based on a parametric formulation of the input and output matrices and application of parametric model reduction. In the second approach, we approximate the time-varying input matrix in a low-dimensional subspace and perform model reduction of a time-invariant system. Both approaches are compared for a thin-walled cylinder model with a rotating force.

1 Introduction

A more precise modelling of engineering problems leads to models of ever increasing complexity. In computational mechanics, the dynamics of elastic multibody systems (EMBS) composed of rigid and flexible bodies is studied numerically. Such systems have a large number of degrees of freedom if, for example, the finite element method (FEM) [1, 2] is used for considering the deformations. This inevitably leads to extremely large systems of ordinary differential equations or differential-algebraic equations if the motion is restricted by some constraints. The resulting systems demand often huge computational effort. In order to decrease the computational complexity, a large-scale system can be replaced by a reduced-oder model that approximates the dynamical behavior and preserves the structure and physical properties of the original system. This procedure known as model reduction has become very popular in a variety of applications, e.g., [3, 4, 5, 6]. In the last decades, many different model reduction techniques have been developed for linear and nonlinear systems, see the books [7,4,8,9] and the recent survey [10].

In this paper, we consider model order reduction of linear mechanical systems with moving loads. Such systems arise in many practical problems including modelling of working gears, milling processes, crankshafts and cranes [11, 12, 13, 14]. Moving loads can be incorporated into the system via a parameter-dependent input matrix, where the parameter describes the position of the acting force and, in general, depends on the time. Two different simplifications lead to different systems to be reduced. First, we assume that the parameter is time independent. In this case, any parametric model order reduction (PMOR) method [15, 16, 17, 18] can be applied to the resulting system. It is another approach, to consider a linear time-varying (LTV) system, in which only the input and output matrices are time-dependent. For model reduction of such systems, we can use balanced truncation methods developed in [19,20,21]. However, these methods are computationally expensive and storage demanding. Therefore, the development of more efficient model reduction techniques for LTV systems is of great interest. In [22], a model reduction approach for systems with time-varying input matrix has been presented which consists of an approximation of the input matrix in a low-dimensional subspace followed by model reduction of a linear time-invariant (LTI) system with a modified input. In this approach, it is assumed that a trajectory of moving load is known before the simulation. Here, we present a comparison of two model reduction approaches based on PMOR and approximation of the input matrix for a thin-walled cylinder model with a rotating force. Note that systems with moving loads can also be modelled as switched systems consisting of LTI subsystems. Model reduction of such systems has been discussed in [23].

The paper is organized as follows. In Section 2, we introduce the equations of motion of EMBS and formulate a model reduction problem. In Section 3, two different modelling approaches for elastic systems with moving loads are considered and model reduction of the resulting

---

†Institute of Engineering and Computational Mechanics, University of Stuttgart, Pfaffenwaldring 9, 70569 Stuttgart, Germany. Supported by the DFG project EB 195/11-1.

‡Insitute of Mathematics, University of Augsburg, Universitätsstr. 14, 86159 Augsburg, Germany. Supported by the DFG project STY 58/1-1.

systems is discussed. Some results of numerical experiments for a cylinder model are presented in Section 4.

2 Elastic multibody systems and model reduction problem

The dynamics of an EMBS can be modelled using the floating frame of reference formulation [2] by the nonlinear differential equations of motion

$$\begin{bmatrix} m\boldsymbol{I} & m\widetilde{\boldsymbol{c}}^T(\boldsymbol{q}) & \boldsymbol{C}_t^T \\ m\widetilde{\boldsymbol{c}}(\boldsymbol{q}) & \boldsymbol{J}(\boldsymbol{q}) & \boldsymbol{C}_r^T(\boldsymbol{q}) \\ \boldsymbol{C}_t & \boldsymbol{C}_r(\boldsymbol{q}) & \boldsymbol{M}_e \end{bmatrix} \begin{bmatrix} \boldsymbol{a} \\ \boldsymbol{\alpha} \\ \ddot{\boldsymbol{q}} \end{bmatrix} + \begin{bmatrix} \boldsymbol{0} \\ \boldsymbol{0} \\ \boldsymbol{K}_e\boldsymbol{q} + \boldsymbol{D}_e\dot{\boldsymbol{q}} \end{bmatrix} = \begin{bmatrix} \boldsymbol{h}_t \\ \boldsymbol{h}_r \\ \boldsymbol{h}_e \end{bmatrix}. \tag{1}$$

These equations describe the nonlinear rigid body motion with the translational and rotational accelerations $\boldsymbol{a}$ and $\boldsymbol{\alpha}$, respectively, and the linear elastic deformation with the nodal displacement vector $\boldsymbol{q}$. The rigid body is characterized by the mass m, inertia $\boldsymbol{J}$ and center of mass $\widetilde{\boldsymbol{c}}$. The right-hand side contains the acting forces $\boldsymbol{h}_t$, $\boldsymbol{h}_r$ and $\boldsymbol{h}_e$. The rigid and elastic parts in (1) are coupled by the matrices $\boldsymbol{C}_t$ and $\boldsymbol{C}_r(\boldsymbol{q})$. The elastic continuum is considered as a spatially discretized body with the symmetric positive definite mass matrix $\boldsymbol{M}_e \in \mathbb{R}^{N\times N}$, the symmetric semidefinite stiffness matrix $\boldsymbol{K}_e \in \mathbb{R}^{N\times N}$ and the damping matrix $\boldsymbol{D}_e \in \mathbb{R}^{N\times N}$, which is often taken as Rayleigh damping, i.e., $\boldsymbol{D}_e = \alpha\boldsymbol{M}_e + \beta\boldsymbol{K}_e$ with $\alpha, \beta > 0$.

The fine spatial discretization of the elastic body leads to a high dimension N. In this case, model order reduction is needed in order to decrease the computational complexity and speed up the simulations. Thereby, the rigid body part remains unchanged, and only the elastic part is reduced. Consequently, the structure of the EMBS equations of motion (1) is retained allowing the use of efficient solvers especially developed for multibody systems. Decoupling the elastic part from (1) leads to a LTI system

$$\boldsymbol{M}_e\ddot{\boldsymbol{q}} + \boldsymbol{D}_e\dot{\boldsymbol{q}} + \boldsymbol{K}_e\boldsymbol{q} = \boldsymbol{B}_e\boldsymbol{u},$$

where the input $\boldsymbol{u} \in \mathbb{R}^m$ describes the acting forces distributed onto the elastic body by the input matrix $\boldsymbol{B}_e \in \mathbb{R}^{N\times m}$. The problem becomes much more difficult if the acting forces or loads change their position in space. In a more general setting, we obtain a parametric time-varying system

$$\begin{aligned} \boldsymbol{M}_e\ddot{\boldsymbol{q}} + \boldsymbol{D}_e\dot{\boldsymbol{q}} + \boldsymbol{K}_e\boldsymbol{q} &= \boldsymbol{B}_e(\boldsymbol{p}(t))\boldsymbol{u}, \\ \boldsymbol{y} &= \boldsymbol{C}_e(\boldsymbol{p}(t))\boldsymbol{q} \end{aligned} \tag{2}$$

with a time-dependent parameter vector

$$\boldsymbol{p}(t) = [\boldsymbol{p}_{[1]}^T(t), \ldots, \boldsymbol{p}_{[m]}^T(t)]^T,$$

where $\boldsymbol{p}_{[j]}(t)$ describes the position of the j-th force at time $t \in [0,T]$. The second equation in (2) is the output equation, where the output $\boldsymbol{y} \in \mathbb{R}^l$ contains the nodal displacements of interest obtained by using the output matrix $\boldsymbol{C}_e \in \mathbb{R}^{l\times N}$. If the elastic deformation at positions of moving loads is observed, then the output matrix takes the form

$$\boldsymbol{C}_e(\boldsymbol{p}(t)) = \boldsymbol{B}_e^T(\boldsymbol{p}(t)).$$

The goal of model reduction is to approximate system (2) by a reduced-order model

$$\begin{aligned} \widetilde{\boldsymbol{M}}_e\ddot{\widetilde{\boldsymbol{q}}} + \widetilde{\boldsymbol{D}}_e\dot{\widetilde{\boldsymbol{q}}} + \widetilde{\boldsymbol{K}}_e\widetilde{\boldsymbol{q}} &= \widetilde{\boldsymbol{B}}_e(\boldsymbol{p}(t))\boldsymbol{u}, \\ \widetilde{\boldsymbol{y}} &= \widetilde{\boldsymbol{C}}_e(\boldsymbol{p}(t))\widetilde{\boldsymbol{q}}, \end{aligned} \tag{3}$$

with the system matrices $\widetilde{\boldsymbol{M}}_e, \widetilde{\boldsymbol{D}}_e, \widetilde{\boldsymbol{K}}_e \in \mathbb{R}^{r\times r}$, $\widetilde{\boldsymbol{B}}_e \in \mathbb{R}^{r\times m}$, $\widetilde{\boldsymbol{C}}_e \in \mathbb{R}^{l\times r}$ and $r \ll N$. The preservation of the second-order structure and the parameter dependency in the reduced model is essential, because this model has to be coupled back to the rigid body part resulting in the reduced EMBS system, see [24] for detailed descriptions.

3 Model reduction of an elastic body subjected to moving loads

In this section, we present two modelling approaches for elastic systems with moving loads and consider model order reduction of the resulting systems.

3.1 Parametric model order reduction with matrix interpolation

As discussed in [25], the moving load problem can be described by a parametric LTI system

$$\begin{aligned} \boldsymbol{M}_e\ddot{\boldsymbol{q}} + \boldsymbol{D}_e\dot{\boldsymbol{q}} + \boldsymbol{K}_e\boldsymbol{q} &= \boldsymbol{B}_e(\boldsymbol{p})\boldsymbol{u}, \\ \boldsymbol{y} &= \boldsymbol{C}_e(\boldsymbol{p})\boldsymbol{q}, \end{aligned} \tag{4}$$

with a time-independent parameter $\boldsymbol{p}$. Here, the parameter dependency in the input and output matrices is supposed to be affine

$$\boldsymbol{B}_e(\boldsymbol{p}) = \sum_{i=1}^{k} \omega_i(\boldsymbol{p})\boldsymbol{B}_{e,i}, \quad \boldsymbol{C}_e(\boldsymbol{p}) = \sum_{i=1}^{k} \omega_i(\boldsymbol{p})\boldsymbol{C}_{e,i} \tag{5}$$

with $\sum_{i=1}^{k} \omega_i(\boldsymbol{p}) = 1$ and $\omega_i(\boldsymbol{p}_j) = \delta_{ij}$ for $i,j = 1,\ldots,k$, where $\boldsymbol{p}_j$ represents a local parameter value. For model reduction of parametric systems, a variety of techniques, in particular based on interpolation, have been developed [15,26,17,18] and applied to structured systems [25,27,28]. In this paper, only the PMOR technique based on matrix interpolation [29,18] is considered.

First, for given parameters $\boldsymbol{p}_i$, $i = 1,\ldots,k$, a linear model order reduction technique based on Petrov-Galerkin projection is employed to compute the local reduced-order systems

$$\begin{aligned} \widetilde{\boldsymbol{M}}_{e,i}\ddot{\widetilde{\boldsymbol{q}}}_i + \widetilde{\boldsymbol{D}}_{e,i}\dot{\widetilde{\boldsymbol{q}}}_i + \widetilde{\boldsymbol{K}}_{e,i}\widetilde{\boldsymbol{q}}_i &= \widetilde{\boldsymbol{B}}_{e,i}(\boldsymbol{p}_i)\boldsymbol{u}, \\ \widetilde{\boldsymbol{y}}_i &= \widetilde{\boldsymbol{C}}_{e,i}(\boldsymbol{p}_i)\widetilde{\boldsymbol{q}}_i \end{aligned}$$

with the projected system matrices

$$
\begin{aligned}
&\widetilde{\boldsymbol{M}}_{e,i} = \boldsymbol{V}_i^T \boldsymbol{M}_e \boldsymbol{V}_i, \quad \widetilde{\boldsymbol{D}}_{e,i} = \boldsymbol{V}_i^T \boldsymbol{D}_e \boldsymbol{V}_i, \quad \widetilde{\boldsymbol{K}}_{e,i} = \boldsymbol{V}_i^T \boldsymbol{K}_e \boldsymbol{V}_i,\\
&\widetilde{\boldsymbol{B}}_{e,i} = \boldsymbol{V}_i^T \boldsymbol{B}_e(\boldsymbol{p}_i), \quad \widetilde{\boldsymbol{C}}_{e,i} = \boldsymbol{C}_e(\boldsymbol{p}_i)\boldsymbol{V}_i.
\end{aligned} \tag{6}
$$

We use here a one-sided projection in order to preserve the symmetry in the reduced mass, damping and stiffness matrices. For nonsymmetric problems, the two-side projection can be applied. Note that the projection matrices $\boldsymbol{V}_i$ in (6) have the same number r of columns for $i = 1, \ldots, k$. To enable the interpolation of the resulting systems, the independently calculated reduced state vectors $\widetilde{\boldsymbol{q}}_i$ have to be transformed to $\widetilde{\boldsymbol{q}}_i^* = \boldsymbol{T}_i^{-1}\widetilde{\boldsymbol{q}}_i$ with

$$
\boldsymbol{T}_i^{-1} = \boldsymbol{R}^T \boldsymbol{V}_i \quad \text{and} \quad \boldsymbol{R}^T \boldsymbol{R} = \boldsymbol{I}.
$$

This guarantees that the reduced systems are described in the same set of coordinates

$$
\widetilde{\boldsymbol{q}}_1^* = \ldots = \widetilde{\boldsymbol{q}}_k^* = \widetilde{\boldsymbol{q}}^*.
$$

In order to determine the matrix $\boldsymbol{R}$, all projection matrices $\boldsymbol{V}_i$ are combined to a matrix $\boldsymbol{V}_{\text{all}} = [\boldsymbol{V}_1, \ldots, \boldsymbol{V}_k]$ and the singular value decomposition $\boldsymbol{V}_{\text{all}} = \boldsymbol{U}\boldsymbol{\Sigma}\boldsymbol{V}^T$ is computed. Then $\boldsymbol{R} = \boldsymbol{U}(:, 1:r)$ is constructed by the r left singular vectors corresponding to the r largest singular values of $\boldsymbol{V}_{\text{all}}$. The transformed local reduced-order system has the form

$$
\begin{aligned}
\widetilde{\boldsymbol{M}}_i \ddot{\widetilde{\boldsymbol{q}}}^* + \widetilde{\boldsymbol{D}}_i \dot{\widetilde{\boldsymbol{q}}}^* + \widetilde{\boldsymbol{K}}_i \widetilde{\boldsymbol{q}}^* &= \widetilde{\boldsymbol{B}}_i \boldsymbol{u},\\
\widetilde{\boldsymbol{y}}_i &= \widetilde{\boldsymbol{C}}_i \widetilde{\boldsymbol{q}}^*
\end{aligned} \tag{7}
$$

with

$$
\begin{aligned}
&\widetilde{\boldsymbol{M}}_i = \boldsymbol{T}_i^T \bar{\boldsymbol{M}}_{e,i} \boldsymbol{T}_i, \quad \widetilde{\boldsymbol{D}}_i = \boldsymbol{T}_i^T \bar{\boldsymbol{D}}_{e,i} \boldsymbol{T}_i, \quad \widetilde{\boldsymbol{K}}_i = \boldsymbol{T}_i^T \bar{\boldsymbol{K}}_{e,i} \boldsymbol{T}_i,\\
&\widetilde{\boldsymbol{B}}_i = \boldsymbol{T}_i^T \bar{\boldsymbol{B}}_{e,i}, \qquad \widetilde{\boldsymbol{C}}_i = \bar{\boldsymbol{C}}_{e,i} \boldsymbol{T}_i.
\end{aligned}
$$

This additional transformation enables a direct interpolation between the reduced system matrices

$$
\begin{aligned}
&\widetilde{\boldsymbol{M}}(\boldsymbol{p}) = \sum_{i=1}^{k} \omega_i(\boldsymbol{p}) \widetilde{\boldsymbol{M}}_i, \quad \widetilde{\boldsymbol{D}}(\boldsymbol{p}) = \sum_{i=1}^{k} \omega_i(\boldsymbol{p}) \widetilde{\boldsymbol{D}}_i,\\
&\widetilde{\boldsymbol{K}}(\boldsymbol{p}) = \sum_{i=1}^{k} \omega_i(\boldsymbol{p}) \widetilde{\boldsymbol{K}}_i,\\
&\widetilde{\boldsymbol{B}}(\boldsymbol{p}) = \sum_{i=1}^{k} \omega_i(\boldsymbol{p}) \widetilde{\boldsymbol{B}}_i, \quad \widetilde{\boldsymbol{C}}(\boldsymbol{p}) = \sum_{i=1}^{k} \omega_i(\boldsymbol{p}) \widetilde{\boldsymbol{C}}_i
\end{aligned} \tag{8}
$$

because all individually reduced systems contain the reduced coordinates $\widetilde{\boldsymbol{q}}^*$. Therefore, the parameter dependency in (5) is retained in the reduced system. Note that although the original parameter-dependent system only contains variations in the input and output matrices, all reduced system matrices vary with the parameter because of the parameter-dependent projection matrices.

3.2 Approximation of the input matrix

Another model reduction approach for mechanical systems with moving loads was proposed in [22]. It exploits the special structure of the input matrix $\boldsymbol{B}_e(\boldsymbol{p}(t))$ in the spatially discretized system. This matrix can be written as

$$
\boldsymbol{B}_e(\boldsymbol{p}(t)) = \left[\boldsymbol{b}(\boldsymbol{p}_{[1]}(t)), \ldots, \boldsymbol{b}(\boldsymbol{p}_{[m]}(t)) \right],
$$

where the components of $\boldsymbol{b} = [\varphi_1, \ldots, \varphi_N]^T$ are the FEM test functions and $\boldsymbol{p}_{[j]}(t)$ describes the position of the j-th force. The model reduction approach consists of two steps. In the first step, the input matrix $\boldsymbol{B}_e(\boldsymbol{p}(t))$ is approximated by

$$
\boldsymbol{B}_e(\boldsymbol{p}(t)) \approx \widehat{\boldsymbol{B}}_e \boldsymbol{\Psi}(\boldsymbol{p}(t)),
$$

where $\widehat{\boldsymbol{B}}_e \in \mathbb{R}^{N \times n}$ with $n \ll N$ is a constant matrix and $\boldsymbol{\Psi}(\boldsymbol{p}(t)) \in \mathbb{R}^{n \times m}$ has the form

$$
\boldsymbol{\Psi}(\boldsymbol{p}(t)) = \left[\boldsymbol{\psi}(\boldsymbol{p}_{[1]}(t)), \ldots, \boldsymbol{\psi}(\boldsymbol{p}_{[m]}(t)) \right] \tag{9}
$$

with an appropriately chosen vector-valued function $\boldsymbol{\psi}(\boldsymbol{p}_{[j]}(t))$. Introducing a new input $\widehat{\boldsymbol{u}}(t) = \boldsymbol{\Psi}(\boldsymbol{p}(t))\boldsymbol{u}(t)$, we obtain the system

$$
\boldsymbol{M}_e \ddot{\widehat{\boldsymbol{q}}} + \boldsymbol{D}_e \dot{\widehat{\boldsymbol{q}}} + \boldsymbol{K}_e \widehat{\boldsymbol{q}} = \widehat{\boldsymbol{B}}_e \widehat{\boldsymbol{u}}, \tag{10}
$$

$$
\widehat{\boldsymbol{y}} = \boldsymbol{C}_e(\boldsymbol{p}(t)) \widehat{\boldsymbol{q}} \tag{11}
$$

with the time-independent input matrix $\widehat{\boldsymbol{B}}_e$. Analogously, we can also approximate the output matrix that gives rise to additional errors in the output. Since in the following description only one-sided projection is used, we do not pursue this further. In the second step, we compute the reduced-order model

$$
\widetilde{\boldsymbol{M}}_e \ddot{\widetilde{\boldsymbol{q}}} + \widetilde{\boldsymbol{D}}_e \dot{\widetilde{\boldsymbol{q}}} + \widetilde{\boldsymbol{K}}_e \widetilde{\boldsymbol{q}} = \widetilde{\boldsymbol{B}}_e \widehat{\boldsymbol{u}}, \tag{12}
$$

$$
\widetilde{\boldsymbol{y}} = \widetilde{\boldsymbol{C}}_e(\boldsymbol{p}(t)) \widetilde{\boldsymbol{q}}, \tag{13}
$$

where

$$
\begin{aligned}
&\widetilde{\boldsymbol{M}}_e = \boldsymbol{V}^T \boldsymbol{M}_e \boldsymbol{V}, \quad \widetilde{\boldsymbol{D}}_e = \boldsymbol{V}^T \boldsymbol{D}_e \boldsymbol{V}, \quad \widetilde{\boldsymbol{K}}_e = \boldsymbol{V}^T \boldsymbol{K}_e \boldsymbol{V},\\
&\widetilde{\boldsymbol{B}}_e = \boldsymbol{V}^T \widehat{\boldsymbol{B}}_e, \qquad \widetilde{\boldsymbol{C}}_e(\boldsymbol{p}(t)) = \boldsymbol{C}_e(\boldsymbol{p}(t)) \boldsymbol{V}
\end{aligned}
$$

with the projection matrix $\boldsymbol{V} \in \mathbb{R}^{N \times r}$ determined by some structure-preserving model reduction method like SOAR [30], MIRA [31] or SO-IRKA [32].

An advantage of the presented two-step model reduction approach is that there is an error bound composed of the error bounds at the approximation and model reduction steps. For the matrix-valued functions

$$
\boldsymbol{F} : [a, b] \to \mathbb{R}^{N \times m}, \qquad \boldsymbol{H} : \mathbb{C} \to \mathbb{C}^{N \times m},
$$

we define the following norms

$$\|\boldsymbol{F}\|_{\mathcal{L}_2(a,b)} = \left(\int_a^b \|\boldsymbol{F}(t)\|_2^2\, dt\right)^{1/2},$$
$$\|\boldsymbol{F}\|_{\mathcal{L}_\infty(a,b)} = \sup_{t\in[a,b]} \|\boldsymbol{F}(t)\|_2,$$
$$\|\boldsymbol{H}\|_{\mathcal{H}_2} = \left(\int_{-\infty}^{\infty} \|\boldsymbol{H}(i\omega)\|_F^2\, d\omega\right)^{1/2},$$
$$\|\boldsymbol{H}\|_{\mathcal{H}_\infty} = \sup_{\omega\in\mathbb{R}} \|\boldsymbol{H}(i\omega)\|_2,$$

where $i=\sqrt{-1}$ is the imaginary unit, $\|\cdot\|_2$ denotes the spectral matrix norm, and $\|\cdot\|_F$ denotes the Frobenius matrix norm. Let

$$\widehat{\boldsymbol{H}}(s) = (s^2\boldsymbol{M}_e + s\boldsymbol{D}_e + \boldsymbol{K}_e)^{-1}\widehat{\boldsymbol{B}}_e,$$
$$\widetilde{\boldsymbol{H}}(s) = \boldsymbol{V}(s^2\widetilde{\boldsymbol{M}}_e + s\widetilde{\boldsymbol{D}}_e + \widetilde{\boldsymbol{K}}_e)^{-1}\widetilde{\boldsymbol{B}}_e,$$

be the transfer functions of (10) with the output $\widehat{\boldsymbol{y}}_* = \widehat{\boldsymbol{q}}$ and of (12) with the output $\widetilde{\boldsymbol{y}}_* = \boldsymbol{V}\widetilde{\boldsymbol{q}}$, respectively. Then we have the error bounds

$$\begin{aligned}\|\boldsymbol{y}-\widetilde{\boldsymbol{y}}\|_{\mathcal{L}_2(0,T)} &\le c_2\,\|\boldsymbol{B}_e(\boldsymbol{p}) - \widehat{\boldsymbol{B}}_e\boldsymbol{\Psi}(\boldsymbol{p})\|_{\mathcal{L}_2(0,T)}\|\boldsymbol{u}\|_{\mathcal{L}_\infty(0,T)}\\ &\quad + \gamma\|\widehat{\boldsymbol{H}} - \widetilde{\boldsymbol{H}}\|_{\mathcal{H}_\infty}\|\widehat{\boldsymbol{u}}\|_{\mathcal{L}_2(0,\infty)},\\ \|\boldsymbol{y}-\widetilde{\boldsymbol{y}}\|_{\mathcal{L}_\infty(0,T)} &\le c_\infty\|\boldsymbol{B}_e(\boldsymbol{p}) - \widehat{\boldsymbol{B}}_e\boldsymbol{\Psi}(\boldsymbol{p})\|_{\mathcal{L}_\infty(0,T)}\|\boldsymbol{u}\|_{\mathcal{L}_\infty(0,T)}\\ &\quad + \gamma\|\widehat{\boldsymbol{H}} - \widetilde{\boldsymbol{H}}\|_{\mathcal{H}_2}\|\widehat{\boldsymbol{u}}\|_{\mathcal{L}_2(0,\infty)}\end{aligned}$$

with some constants $c_2, c_\infty, \gamma > 0$, see [22] for details. These error bounds imply that small approximation errors in the input matrix and small model reduction errors lead to small errors in the output $\widetilde{\boldsymbol{y}}$ of the reduced-order model (12), (13).

This suggests to reformulate the approximation problem for the input matrix as a continuous linear least squares (LLS) minimization problem: Given a vector-valued function $\boldsymbol{\psi}$, find a matrix $\widehat{\boldsymbol{B}}_e \in \mathbb{R}^{N\times n}$ which minimizes the $\mathcal{L}_2$-norm error

$$\|\boldsymbol{B}_e(\boldsymbol{p}) - \widehat{\boldsymbol{B}}_e\boldsymbol{\Psi}(\boldsymbol{p})\|_{\mathcal{L}_2(0,T)} = \left(\int_0^T \|\boldsymbol{B}_e(\boldsymbol{p}(t)) - \widehat{\boldsymbol{B}}_e\boldsymbol{\Psi}(\boldsymbol{p}(t))\|_2 dt\right)^{1/2}$$

with $\boldsymbol{\Psi}$ as in (9). Assuming that the force position vector $\boldsymbol{p}$ is known on the time interval $[0,T]$ and taking into account the structure of the columns of $\boldsymbol{B}_e$, the components of $\boldsymbol{\psi}$ can be chosen as Legendre polynomials or as FEM test functions on a coarse grid, see [22] for a detailed description.

4 Numerical experiments

In this section, we present the comparison results for the considered model reduction approaches applied to a thin-walled cylinder with a rotating force described in [11]. For solving the nonlinear EMBS in the time domain, we use the multibody simulation code Neweul-M^2 [33], whereas the reduced-order models were computed using MATLAB.

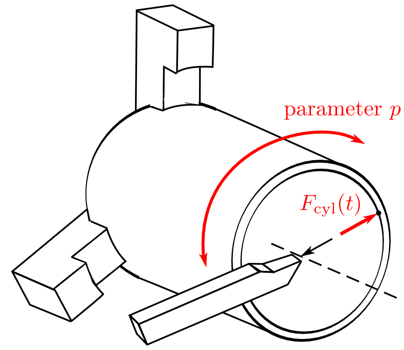

Fig. 1. A thin-walled cylinder model with the rotating contact force $F_{\mathrm{cyl}}(t)$

4.1 Mechanical model

To simulate the turning of a thin-walled cylinder in an EMBS environment, highly accurate descriptions of the elastic behavior are indispensable [11]. The force between the cylinder and the tool changes its position, meaning that each node on the surface might be actuated in the simulation model. Figure 1 shows the thin-walled cylinder with the contact force $F_{\mathrm{cyl}}(t)$ modelled as a point force. Observing the displacement at the position of the rotating force, we obtain a single-input single-output system. For easier comparison of the two presented descriptions of the load movement, the cylinder is fixed and the force is rotating inside the cylinder. A single parameter p describes the angular position of the force around the circumference at the tip of the cylinder. The finite element model consists of 180 nodes around the circumference and 82 nodes in longitudinal direction. Each node contains three translational degrees of freedom. After removing rigidly fixed nodes, we get $N = 43983$ independent degrees of freedom. The magnitude of the frequency response $|H(i2\pi f)|$ of the cylinder model with the input and output node at the tip is depicted in Figure 2 for the frequency range $[0,\ 3000]$ Hz.

4.2 Reference solution with various model reduction techniques

The original elastic body cannot be calculated in the EMBS environment due to the large amount of elastic degrees of freedom. Hence, the reference solution is generated with the classical EMBS approach based on the Component Mode Synthesis (CMS) with a combination of two sets of modes. Thereby, a certain number of eigenmodes represents the harmonic behavior of the elastic body and the static deformation is described by static modes. For each possibly actuated node and direction, one static mode is calculated. In this example, this leads to 3×180 static modes for all nodes around the circumference and three translational degrees of freedom. Additional 10 eigenmodes already deliver very satisfying results in the frequency domain, see [34]. To

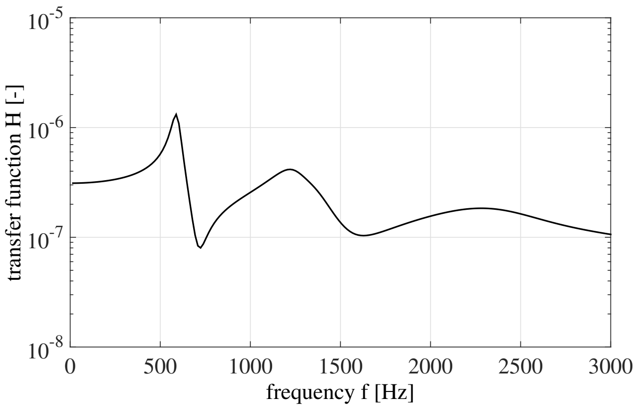

Fig. 2. Frequency response $H(i2\pi f)$ of the cylinder model

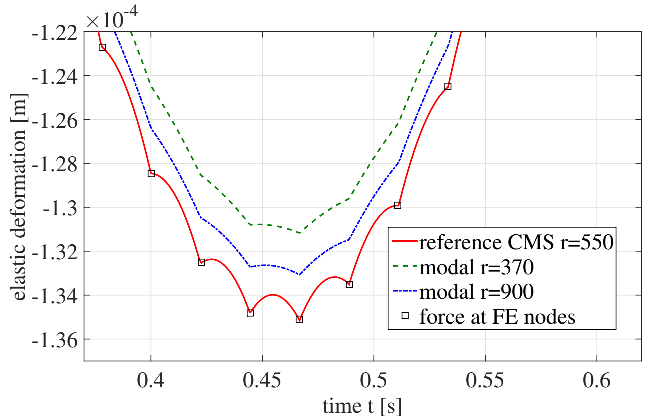

Fig. 4. Elastic deformation of moved marker for modally reduced systems in comparison with the reference solution

check the quality of the obtained reference system, a second reduced-order model with $r = 1068$ degrees of freedom is determined by applying a block-Arnoldi algorithm with expansion points at $f = 0\,\text{Hz}$ and $f = 500\,\text{Hz}$ to the original system with all possible inputs. This leads to an extremely small relative error in the frequency domain for the both reference systems. Figure 3 illustrates the elastic deformation for the reference solutions. Both reference configurations show the same behavior. If the force acts between two nodes of the finite element mesh, the projection matrix is determined by interpolation of the information at the neighboring nodes. Due to the fact that the nodes do not contain rotational degrees of freedom and the local finite element shape functions are linear, the results show nonphysical heightening between the nodes. This behavior does not come from the physics of the system but rather from the discretization.

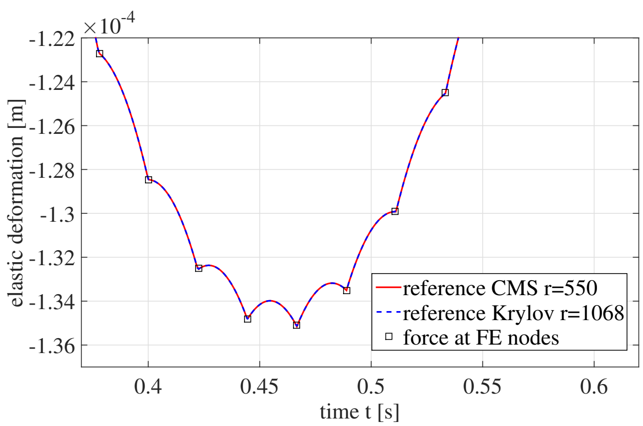

Fig. 3. Elastic deformation of the moved marker for two reference solutions

One model reduction approach without concerning the acting forces in model reduction is the modal truncation. The unsatisfactory quality of modally reduced systems is depicted in Figure 4 for two reduction dimensions $r = 370$ and $r = 900$.

We also examine a model reduction technique which will be combined later on with the approximation of the input matrix. For this purpose, we apply a modification of the SO-IRKA [32] presented in [22] to the system with the not approximated input matrix. To improve the approximation properties of the reduced model, we repeat the modified SO-IRKA with random initial values to get the projection matrices $\boldsymbol{V}_1, \ldots, \boldsymbol{V}_s$ and compute the singular value decomposition of $[\boldsymbol{V}_1, \ldots, \boldsymbol{V}_s]$ to obtain a final projection matrix. Compared to the modally truncated model of order $r = 900$, the Krylov-reduced system even with $r = 150$ degrees of freedom represents the original dynamics better, see Figure 5. The reduced model of order $r = 520$ is very close to the reference solution. Note that still a large number of reduced elastic degrees of freedom is necessary to generate qualitatively satisfying reduced elastic bodies.

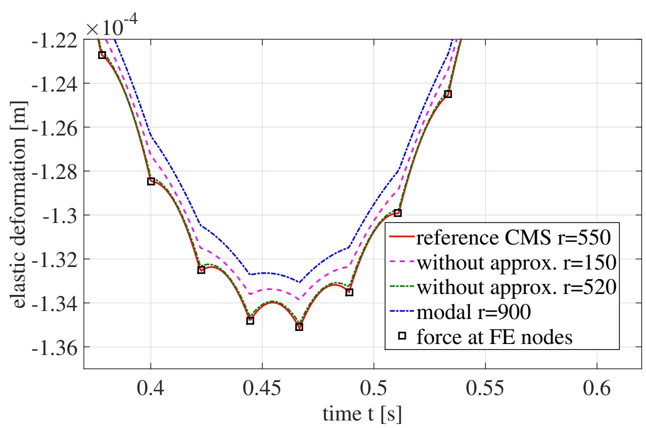

Fig. 5. Elastic deformation of moved marker for the reduced models computed by the modified SO-IRKA in comparison with the reference solution and the modal reduced system

4.3 Comparison of two model reduction approaches

We verify now two model reduction approaches for systems with moving load presented in Section 3.

In PMOR, the local reduced systems are generated with the CMS approach with 10 eigenmodes and one static mode. The static mode is chosen with the knowledge about the position of the acting force and the direction of the force orthogonal to the surface of the cylinder. This is equivalent to the sampling of the parameter space by using each possible support system. In the preparation of the local reduced systems in the offline step, the correct input, which will appear in the simulation of the moving load at the corresponding node, is considered. In the online step, piecewise linear interpolation of the reduced system matrices is performed, because the local finite element shape functions are linear. Higher order interpolation schemes, like cubic spline interpolation, improve these results and require less sampled systems, see [25] for detailed results.

The LLS approximation problem for the input matrix is solved using two types of basis functions: the Legendre polynomials [35] and the FEM cubic test functions [36] on a coarse grid. The position of the rotating force is described by a linear function with a constant angular velocity. For model reduction of the approximated systems with $n = 180$ inputs, we employ the modified SO-IRKA as described in the previous subsection.

The results for the different approximation methods for the input matrix are given in Figure 6. The approximated and reduced models contain nearly the same number of reduced elastic degrees of freedom. It is not possible to determine a superior method for these reduction sizes because both models show a very similar behavior. For comparison, we also present in Figure 6 the results for the reduced-order model obtained by the interpolation of the local reduced system matrices. Due to the relatively slow movement of the acting force, the results of the interpolated system are exact, when the force is acting at the finite element nodes. If the force acts between the nodes, the interpolated reduced system does not show the distinctive heightening because all information of the reduced system, including the system matrices, are interpolated.

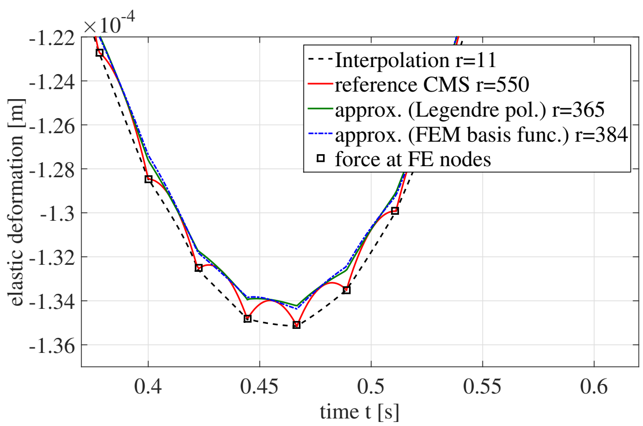

Fig. 6. Elastic deformation of moved marker for the interpolated reduced system and two approximated and reduced systems in comparison with the reference solution

The reduced systems with more than 350 degrees of freedom generated by the approximation of the input matrix are relatively large and it is interesting to consider systems of smaller dimension. Therefore, the approximated systems are reduced to $r = 100$ and compared among themselves and the systems obtained by other methods. The deformations of the reduced systems without approximation of the input matrix are depicted in Figure 7. One can see that the reduction without approximation provides reduced models with nearly the same quality as modally reduced systems with nine times the number of elastic degrees of freedom. This shows the large benefit regarding the inputs although an exact solution at the FE nodes is not achievable with one representative model with $r = 100$.

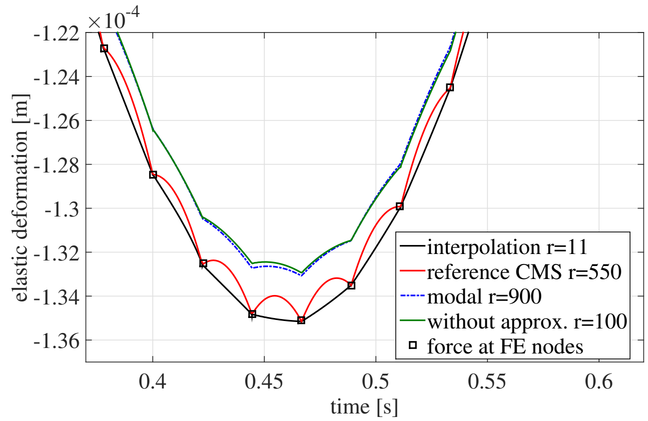

Fig. 7. Elastic deformation of moved marker for the system without approximation of the input matrix reduced by the modified SO-IRKA to the smaller dimension in comparison with the interpolated reduced system, the modally reduced system and the reference solution

The input approximation combined with model reduction leads to the results in Figure 8. The Legendre polynomial approximation shows worse results than the approximation based on the FEM basis functions. The fact that model reduction without approximation and with the LLS approximation of the input matrix gives similar results means that the error of model reduction exceeds the approximation error. This shows once again that the quality of reduced mechanical systems with moving pointal loads highly depends on the inputs. Therefore, it is very difficult to determine systems with few degrees of freedom which represent the dynamics for all inputs.

5 Conclusion

In this paper, we have presented two model reduction approaches for elastic bodies with moving loads. Such problems lead to large systems with the input and output matrices depending on a time-varying parameter describing the position of the acting forces. In the first approach, we have assumed that the parameter is time-independent and applied the parametric model reduction method based on matrix interpo-

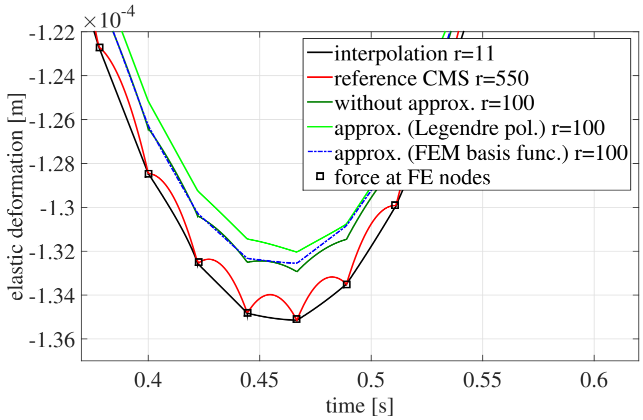

Fig. 8. Elastic deformation of moved marker for smaller reduced systems with and without approximation of the input matrix in comparison with the interpolated reduced system and the reference solution

lation [18]. In the second approach, we have supposed that the force position is known yielding a parameter-independent system with the time-varying input and output matrices. The input matrix was approximated in the least squares sense providing an approximate system with a time-invariant input matrix. Thereby, it is important to keep the number of columns in the new input matrix as small as possible. The resulting system was then approximated by a reduced-order model using the modified SO-IRKA.

The both approaches were examined for the model of the thin-walled cylinder with a rotating force. On the one hand, the parametric interpolation method shows excellent results for the very small reduced models. On the other hand, the approach based on the input matrix approximation can determine a system which provides qualitatively satisfying reduced system without any necessity of interpolation. Often, a higher number of elastic degrees of freedom are necessary. Thus, the both model reduction methods are of interest in the simulation of elastic systems subjected to moving loads.

In future developments, moving loads and interactions in elastic multibody systems including rigid body motions will be investigated.

6 Acknowledgments

The authors gratefully thank the German Research Foundation (DFG) for the support of this research work within the project EB 195/11-1 and STY 58/1-1.

References

[1] Géradin, M., and Cardona, A., 2000. *Flexible Multibody Dynamics. A Finite Element Approach*. John Wiley & Sons, Ltd, Chichester.

[2] Shabana, A., 2005. *Dynamics of Multibody Systems*. Cambridge University Press, Cambridge.

[3] Bechtold, T., Korvink, J., and Rudnyi, E., 2007. *Fast Simulation of Electro-Thermal MEMS: Efficient Dynamic Compact Models*. Microtechnology and MEMS. Springer-Verlag, Berlin.

[4] Benner, P., ed., 2015. *System Reduction for Nanoscale IC Design*, Vol. 20 of *Mathematics in Industry*. Springer-Verlag, Berlin.

[5] Fehr, J., 2011. "Automated and error controlled model reduction in elastic multibody systems". Doctoral thesis, Universität Stuttgart, Shaker Verlag, Aachen.

[6] Ravindran, S., 2000. "A reduced-order approach for optimal control of fluids using proper orthogonal decomposition". *Internat. J. Numer. Methods Fluids,* **34**(5), pp. 425–448.

[7] Antoulas, A., 2005. *Approximation of Large-Scale Dynamical Systems*. SIAM, Philadelphia, PA.

[8] Quarteroni, A., and Rozza, G., eds., 2014. *Reduced Order Methods for Modeling and Computational Reduction*, Vol. 9 of *Modeling, Simulation and Applications*. Springer-Verlag, Berlin.

[9] Schilders, W., van der Vorst, H., and Rommes, J., eds., 2008. *Model Order Reduction: Theory, Research Aspects and Applications*, Vol. 13 of *Mathematics in Industry*. Springer-Verlag, Berlin.

[10] Baur, U., Benner, P., and Feng, L., 2014. "Model order reduction for linear and nonlinear systems: A system-theoretic perspective". *Arch. Comput. Methods Engng.,* **21**(4), pp. 331–358.

[11] Fischer, A., and Eberhard, P., 2011. "Simulation-based stability analysis of a thin-walled cylinder during turning with improvements using an adaptronic turning chisel". *Arch. Mech. Engng.,* **58**(4), pp. 367–391.

[12] Ouyang, H., 2011. "Moving-load dynamic problems: A tutorial (with a brief overview)". *Mech. Systems Signal Processing,* **25**(6), pp. 2039–2060.

[13] Wang, J., and Howard, I., 2005. "Finite element analysis of high contact ratio spur gears in mesh". *J. Tribology,* **127**, pp. 469–483.

[14] Zrnić, N., Gašić, V., Bošnjak, S., and Đorđević, M., 2013. "Moving loads in structural dynamics of cranes: bridging the gap between theoretical and practical researches". In Proceedings of the 11-th International Conference on Vibration Problems (ICOVP 2013, Lisbon, Portugal, September 9-12, 2013), paper 79_0.

[15] Amsallem, D., and Farhat, C., 2008. "Interpolation method for adapting reduced-order models and application to aeroelasticity". *AIAAJ,* **46**(7), pp. 1803–1813.

[16] Baur, U., Beattie, C., Benner, P., and Gugercin, S., 2011. "Interpolatory projection methods for parameterized model reduction". *SIAM J. Sci. Comput.,* **33**(5), pp. 2489–2518.

[17] Benner, P., Gugercin, S., and Willcox, K., 2013. A survey of model reduction methods for parametric systems. Tech. Rep. MPIMD/13-14, Max Planck Institute, Magdeburg. Available from http://www.mpi-magdeburg.mpg.de/preprints/.

[18] Panzer, H., Mohring, J., Eid, R., and Lohmann, B., 2010. "Parametric model order reduction by matrix interpolation". *at-Automatisierungstechnik,* **58**(8), pp. 475–484.

[19] Sandberg, H., and Rantzer, A., 2004. "Balanced truncation of linear time-varying systems". *IEEE Trans. Automat. Control,* **49**(2), pp. 217–229.

[20] Shokoohi, S., Silverman, L., and Van Dooren, P., 1983. "Linear time-variable systems: balancing and model reduction". *IEEE Trans. Automat. Control,* **28**(3), pp. 810–822.

[21] Verriest, E., 2008. "Time variant balancing and nonlinear balanced realizations". In *Model Order Reduction: Theory, Research Aspects and Applications*, W. Schilders, H. van der Vorst, and J. Rommes, eds., Vol. 13 of *Mathematics in Industry*. Springer-Verlag, Berlin, Heidelberg, pp. 213–250.

[22] Stykel, T., and Vasilyev, A., 2015. Model reduction for mechanical systems subjected to moving loads. Preprint, Universität Augsburg.

[23] Lang, N., Saak, J., and Benner, P., 2014. "Model order reduction for systems with moving loads". *at-Automatisierungstechnik,* **62**(7), pp. 512–522.

[24] Lehner, M., 2007. Modellreduktion in elastischen Mehrkörpersystemen. Vol. 10 of Dissertation, Schriften aus dem Institut für Technische und Numerische Mechanik der Universität Stuttgart, Aachen. (in German).

[25] Fischer, M., and Eberhard, P. "Application of parametric model reduction with matrix interpolation for simulation of moving loads in elastic multibody systems". *Adv. Comput. Math.* accepted for publication, DOI:10.1007/s10444-014-9379-7.

[26] Amsallem, D., and Farhat, C., 2011. "An online method for interpolating linear parametric reduced-order models". *SIAM J. Sci. Comput.,* **33**(5), pp. 2169–2198.

[27] Fischer, M., and Eberhard, P., 2014. "An overview about parametric model reduction for mechanical systems with moving loads". In Proceedings of the GMA Working Group 1.30/1.40 (Anif, September 22-23, 2014).

[28] Son, N., and Stykel, T., 2014. Model order reduction of parameterized circuit equations based on interpolation. Preprint 01/2014, Universität Augsburg. Available from http://opus.bibliothek.uni-augsburg.de/opus4/frontdoor/index/index/docId/2583.

[29] Geuss, M., Panzer, H., and Lohmann, B., 2013. "On parametric model order reduction by matrix interpolation". In Proceedings of the European Control Conference (Zürich, Switzerland, July 17-19, 2013), IEEE, pp. 3433–3438.

[30] Bai, Z., and Su, Y., 2005. "Dimension reduction of large-scale second-order dynamical systems via a second-order Arnoldi method". *SIAM J. Sci. Comp.,* **26**, pp. 1692–1709.

[31] Soppa, A., 2011. "Krylov-Unterraum basierte Modellreduktion zur Simulation von Werkzeugmaschinen". Doctoral thesis, Technische Universität Braunschweig.

[32] Wyatt, S., 2012. "Issues in interpolatory model reduction: Inexact solves, second-order systems and DAEs". Ph.D. thesis, Virginia Polytechnic Institute.

[33] Kurz, T., and Eberhard, P., 2011. "Flexible bodies in symbolic multibody systems with Neweul-M2". In *Advanced Applications and Perspectives of Multibody System Dynamics, Proceedings of the the EUROMECH Colloquium 515 (July 13-16, 2010, Blagoevgrad, Bulgaria)*, E. Zahariev and M. Ceccarelli, eds. Bulgarian Academy of Sciences, pp. 48–49.

[34] Fischer, M., and Eberhard, P., 2014. "Simulation of moving loads in elastic multibody systems with parametric model reduction techniques". *Arch. Mech. Engng,* **61**(2), pp. 209–226.

[35] Osilenker, B., 1999. *Fourier Series in Orthogonal Polynomials*. World Scientific Publishing Co. Pte. Ltd., Singapore.

[36] Becker, E., Carey, G., and Oden, J., 1981. *Finite Elements: An Introduction*. Prentice-Hall, Englewood Cliffs.